GEOPHYSICAL RESEARCH LETTERS, VOL. 34, L20804, doi:10.1029/2007GL031518, 2007

Enhanced ionospheric ELF/VLF generation efficiency by multiple timescale modulated heating

G. M. Milikh[1] and K. Papadopoulos[1]

Received 30 July 2007; revised 30 August 2007; accepted 7 September 2007; published 20 October 2007.

[1] It is shown theoretically that for high power HF ionospheric heaters, such as the current HAARP heater, the HF to VLF conversion can increase significantly by using a two-timescale heating. A long heating pulse, $t_p \approx 1$ minute, is followed over the same timescale period by modulation at the desired ELF/VLF frequency. The long pulse reduces the electron-ion recombination coefficient, resulting in increased ambient electron density and current density. The efficiency increases due to the increase in the current density over the time t_p. Besides, the more efficient heating results from sharpening of the ambient density profile at the modified height that reduces low altitude self-absorption. It is shown that following the long preheating pulse by amplitude modulated heating at VLF frequencies can result in efficiency increase of up to 7 dB over the non-preheated case. In addition to the theory the letter describes proof-of-principle experiments using the completed HAARP. **Citation:** Milikh, G. M., and K. Papadopoulos (2007), Enhanced ionospheric ELF/VLF generation efficiency by multiple timescale modulated heating, *Geophys. Res. Lett.*, *34*, L20804, doi:10.1029/2007GL031518.

1. Introduction

[2] The generation of ELF/VLF waves by modulated heating of the lower auroral ionosphere has been the subject of numerous theoretical [*Tripathi et al.*, 1982; *Papadopoulos et al.*, 1989, 1990; *Zhou et al.*, 1996] and experimental [*Barr and Stubbe*, 1984, 1991; *Rietveld et al.*, 1986, 1987; *Ferraro et al.*, 1989; *McCarrick et al.*, 1990; *Milikh et al.*, 1999; *Mironenko et al.*, 1998; *Papadopoulos et al.*, 2003, 2005] investigations. A critical issue in the practical implementation of the technique is the HF to VLF conversion efficiency and its scaling with the increase in the HF power. Straightforward analysis predicts that the conversion efficiency η will scale at least as the square of the HF power P ($\eta \sim P^2$). The scaling issue is a very opportune one since the power of the HAARP heater in Gakona, Alaska has recently increased from the level of 0.96 MW to approximately 3.6 MW. On the basis of this argument we expect that the completed HAARP facility operating at 3.6 MW power will increase the efficiency by approximately 12–14 dB. In this letter we demonstrate theoretically that by using multiple time scale heating the VLF generation efficiency can further increase by 3–7 dB thereby achieving 20 dB overall efficiency increase over the current 0.96 MW operation. In addition to the theory the letter describes proof-of-principle experiments using the completed HAARP.

[3] Before discussing the results and the underlying physics considerations it is important to note that the methodology used to asses the efficiency is based on recent experimental results [*Papadopoulos et al.*, 2005, 2006; *Rietveld et al.*, 1987; *Rietveld and Stubbe*, 2006]. In this work it was demonstrated that the scaling of the conversion efficiency from HF to VLF can be assessed by studying the magnetic response of the lower ionosphere to pulsed HF heating as a function of the heating pulse length t_p = 1/2f. It was further shown by high resolution measurements [*Papadopoulos et al.*, 2005] that the waveform at a frequency f is nothing more that a superposition of the magnetic impulse responses with on-off times t_p = 1/2f. As a result the conversion efficiency for straight vertical heating can be assessed by studying the magnetic impulse response as a function of the heating pulse length.

2. Efficiency Enhancement Physics

[4] The physics of the efficiency enhancement at effective power level can be understood by the following simple considerations. It has been shown that to zero order the value of the magnetic field B measured on the ground scales as [*Papadopoulos et al.*, 2005]

$$B \propto j_0 \, S \, F(\Delta T_e) \qquad (1)$$

where j_0 is the ambient electrojet current density, S is the heated area, and $F(\Delta T_e)$ is a function that describes the part of the conductivity modification (Hall or Pedersen) caused by the HF electron heating. Although it is not a simple linear effect, but the magnetic field B depends on the Hall and Pedersen conductance that are determined by the height profiles of the electron density. Notice that for VLF frequencies corresponding to periodic pulses with lengths shorter than few ms the electron density is essentially constant.

[5] However, this is not the case for long heating pulses. For heating times longer than tens of seconds the resultant electron heating increases the electron density by reducing the electron-ion recombination rate [*Gurevich*, 1978]. Since the current density, as well as the conduction scales linearly with the plasma density, preheating results in increased conversion efficiency. The density enhancement has been experimentally confirmed in artificial ionospheric modification at mid-latitudes, [e.g., *Golyan et al.*, 1982]. The temperature dependence of the recombination rate can be found by noting that the dominant positive ions in the lower ionosphere (z < 85 km) are water cluster ions $H^+(H_2O)_n$. Their electron-ion recombination rate α depends on the

[1]Department of Astronomy, University of Maryland, College Park, Maryland, USA.

0094-8276/07/2007GL031518$05.00

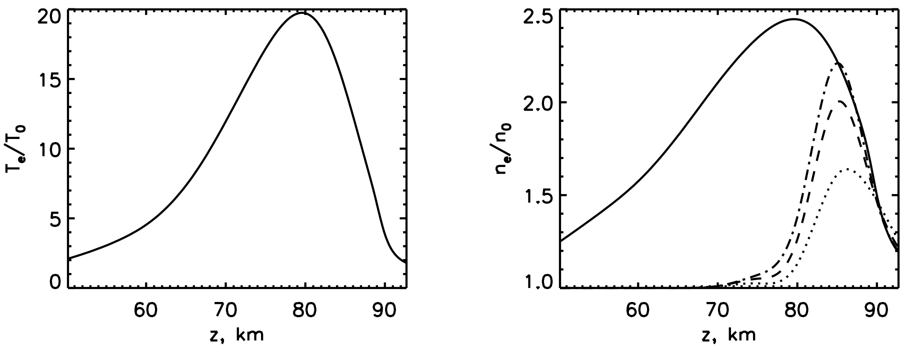

Figure 1. Altitude profiles of the ratio of the (left) perturbed electron temperature and (right) electron density to their respective ambient values. The heating is due to a long HF-pulse of f_{HF} = 4 MHz, X-mode polarization, and ERP = 88.3 dBW in the quiet nighttime auroral ionosphere. Traces from the bottom to the top on Figure 1 (right) correspond to preheating by pulse lengths of 100, 200, 300 s. The solid trace corresponds to the steady state value.

number of water molecules in the cluster, with an average value given by [*Gurevich*, 1978; *Johnsen*, 1993]

$$\alpha = \alpha_0 (300K/T_e)^{0.6}, \quad \alpha_0 = 2.5 \times 10^{-6}\ \mathrm{cm}^3/\mathrm{s} \tag{2}$$

It is important to note that while the density relaxation time is of the order of one minute the temperature relaxation time is only of the order of 10–100 μs.

[6] The above considerations dictate the following strategy for efficiency enhancement using a two-timescale heating. A long heating pulse, $t_p \approx 1$ minute, is followed over the same timescale period by modulation at the desired ELF/VLF frequency $f \gg 1/t_p$. The efficiency increase is the result of the increase in the current density j_0 in equation (1) over the time T_0 and, as shown later on, of the more efficient heating resulting from sharpening of the ambient density profile at the modified height.

[7] A computation of the efficiency increase by two timescale heating requires two steps. First, we compute the density profile expected from long pulse heating as a function of the heater Effective Radiated Power (ERP), ambient ionospheric model, and pulse length. Second, we will use the modified steady density model as input in the code described by *Papadopoulos et al.* [2003, 2005] to determine the amplitude of the impulse response as *a* function of the short pulse length and ionospheric profile as compared to the single time-scale heating. These computations are presented in the next two sections.

3. Density Modification and Heating Pulse-Length Requirement

[8] The steady state level of the modified density profile was computed in two steps: First, the Heater Code (HT) described in detail by *Papadopoulos et al.* [2003] was run to compute the steady state temperature profile. The HT code is a 1-D fluid code that models the absorption of the HF in the ionosphere, the accompanying electron heating, and the modification of the collision frequency and tensor conductivity in a self-consistent manner. Inputs to the code are the electron density profile as a function of altitude, and the heater ERP, frequency, polarization, and heating pulse length. A number of ionospheric profiles similar to the ones discussed by *Rietveld et al.* [1986] are used defined by the observed riometer absorption. Figure 1 (left) shows the steady state altitude profile of the electron temperature for the case of HF-heating at a frequency f_{HF} = 4 MHz, ERP = 88.3 dBW and X-mode polarization. This ERP level is consistent with HAARP heater specifications and is currently available. In this calculation the quiet nighttime ambient ionospheric density profile was used [*Rietveld et al.*, 1986]. In this case the low altitude self-absorption is minimal, providing conditions for the strongest electron density modification. The timescale for achieving steady state electron temperature at the altitude of interest here (<90 km) is of the order of less than ms.

[9] Second, since the timescale for the density modification is of the order of one minute or longer, the density profile is computed by using a quasi-analytic algorithm. Namely by solving the ionization/recombination balance equation

$$\frac{dn_e}{dt} = q - \alpha(T_e) n_e^2, \tag{3}$$

where q is the ambient ionization rate, with the initial condition $n_e(t = 0) = n_0$, and n_0 is the ambient electron density. For $t > 0$, the solution of equation (3) yields

$$n_e(t) = n_0 \sqrt{\frac{\alpha_0}{\alpha_1}} \cdot \frac{\left(1 + \sqrt{\alpha_1/\alpha_0}\right) \exp\left\{2\sqrt{\alpha_0 \alpha_1} n_0 t\right\} - \left(1 - \sqrt{\alpha_1/\alpha_0}\right)}{\left(1 + \sqrt{\alpha_1/\alpha_0}\right) \exp\left\{2\sqrt{\alpha_0 \alpha_1} n_o t\right\} + \left(1 - \sqrt{\alpha_1/\alpha_0}\right)}, \tag{4}$$

where $\alpha_0 = \alpha(T_0)$, $\alpha_1 = \alpha(T_1)$. Using equation (2) the modified electron density profile $n_e(z)$ is obtained for the pulse-width longer than the characteristic timescale of the electron density modification, $\tau_{ch} = 1/\sqrt{\alpha_1 \alpha_0}\ n_0$

$$n_e = n_0 \sqrt{\frac{\alpha_0}{\alpha_1}} \propto \left(\frac{T_e}{T_0}\right)^{0.3} \tag{5}$$

The profiles of the modified electron density corresponding to the parameters and ambient models used in calculating Figure 1 (left) are shown in the right panel of Figure 1 computed for pulse lengths T_0 of 100, 200, and 300 s.

[10] Note that the altitude of maximum density modification is determined by the two height dependent factors, $T_e(z)$ and $\tau_{ch}(z)$, the latter in turn depends upon $n_0(z)$. As revealed by the right panel of Figure 1 at the relatively low heating time the $n(z)$ increases at the altitudes higher than 80 km where the ambient electron density $n_0(z)$ is large and thus the heating time $\tau_{ch}(z)$ is short. When the heating time increases the electron density at the lower altitudes rises. Finally, under very long heating pulse the peak of electron density modification coincides with the peak of the electron temperature. Another important parameter in our analysis is the characteristic timescale required for the density to reach its steady state value as function of altitude shown as a continuous line in Figure 1 (left). The heating length required to reach .9 of its steady state value $n_0\sqrt{\alpha_0/\alpha_1}$ is of τ_{ch}. We computed the pulse length required to reach steady state value as a function of altitude for a quiet, nighttime ionospheric density profile. In fact, for the maximum density modification at 80 km (see Figure 1) the required pre-heating pulse lengths should be between 100–1000 s. Furthermore, since τ_{ch} increases with decreasing altitude, pulses of the order of τ_{ch} at 80 km will produce a sharp density profile such as shown in Figure 1, which will reduce the undesirable nonlinear absorption at the lower altitude.

4. Waveforms in the Presence of Pre-heating

[11] A numerical model that describes ELF/VLF generation has been developed over past several years, and checked against observations [*Papadopoulos et al.*, 2003, 2005]. There are two steps in the computation. The first computes the spatio-temporal profile of the current density $\vec{j}(\vec{r}, t)$ induced by the heater. This is done by using the HT heating code discussed above. The second computes the near field at the observation site, which we take as the origin of the coordinate system, by using the retarded potential method. The vector potential due to an ionospheric current which fills in the volume 2 is

$$\vec{A}(\vec{r},t) = \frac{\mu_0}{4\pi}\int \frac{\vec{j}(2, t - r_{12}/c)}{r_{12}} dV_2 \qquad (6)$$

where μ_0 is permeability of free space, j is the current density, and r_{12} is the distance between the observation point 1 and the integrated volume. Furthermore, the magnetic field generated by the current is given by

$$\vec{B}(\vec{r},t) = \nabla \times \vec{A}(\vec{r},t) \qquad (7)$$

From these equations and assuming an ambient electric field E_0 in the x direction, the Hall (B_x) and Pedersen (B_y) components of magnetic field at the observation point are given by

$$B_x(0,t) = \frac{\mu_0}{4\pi} S E_0 \int \left[\frac{\Delta\sigma_H(z, t - z/c)}{z^2} + \frac{\Delta\dot{\sigma}_H(z, t - z/c)}{cz}\right] dz \qquad (8)$$

$$B_y(0,t) = \frac{\mu_0}{4\pi} S E_0 \int \left[\frac{\Delta\sigma_P(z, t - z/c)}{z^2} + \frac{\Delta\dot{\sigma}_P(z, t - z/c)}{cz}\right] dz \qquad (9)$$

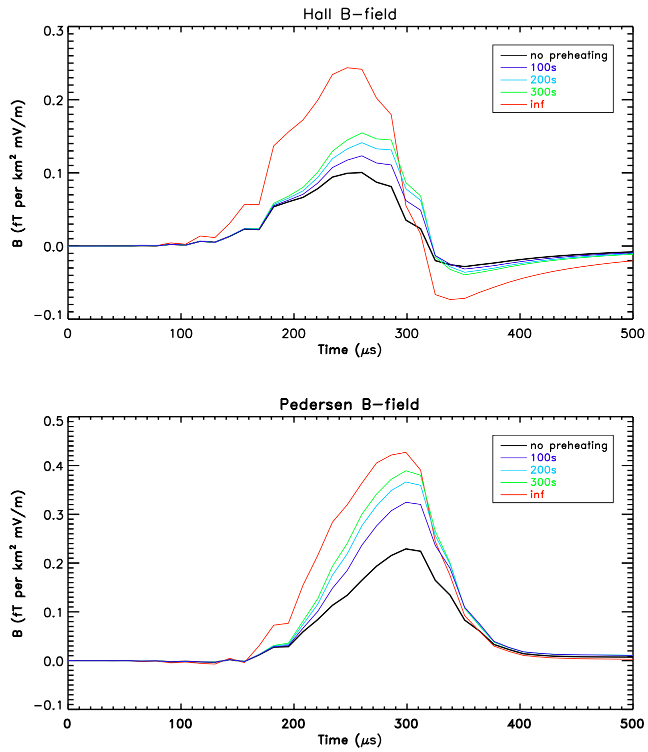

Figure 2. Hall and Pedersen waveforms generated by HF pulse lengths of 100 μs, f_{HF} = 9.0 MHz, ERP = 95.7 dBW, X-mode for quiet nighttime ionospheric profile. The bottom pulses correspond to the absence of preheating, while the remaining pulses by the preheating at of f_{HF} = 4 MHz, ERP = 88.3 dBW, X-mode and pulse lengths of 100, 200, 300 s (from the bottom to the top). The very top trace corresponds to the steady state value.

where $\Delta\sigma_{H,P}$ are perturbations of the Hall and Pedersen conductivities due to the modulated HF-heating, S is the HF heated area, while $\Delta\dot{\sigma}_{P,H}$ represents derivative with respect to the retarded time. Note that the first term in the square brackets in equations (8) and (9) describes the magnetic field due to the ionospheric current induced by the HF heating, while the second term is due to the time derivative of the current. To determine the relative importance of preheating on the efficiency of VLF generation we use the following computational procedure: First use the code to compute the expected VLF waveforms for ambient ionospheric profiles. Then, compute separately the modified density profile due to a long pulse as discussed in Section 3. Finally, rerun the code using the modified electron density profile instead of the ambient one.

[12] Figures 2 (top) and 2 (bottom) show the Hall and Pedersen magnetic field on the ground computed per unit heating area and per unit electric field. They were caused by a pulse of 100 μs length, at f_{HF} = 9 MHz, ERP = 95.7 dBW, and X-mode polarization. The bottom plots in Figure 3 show the waveforms generated without preheating, while the remaining plots correspond to waveforms by preheating at f_{HF} = 4 MHz, ERP = 88.3 dBW, X-mode with the pulse lengths t_p = 100, 200, 300 s. It is seen that increasing the preheating pulse length results in an increase of the VLF pulse that reaches maximum at the steady state value of the modified profile. This effect is due to the fact that the

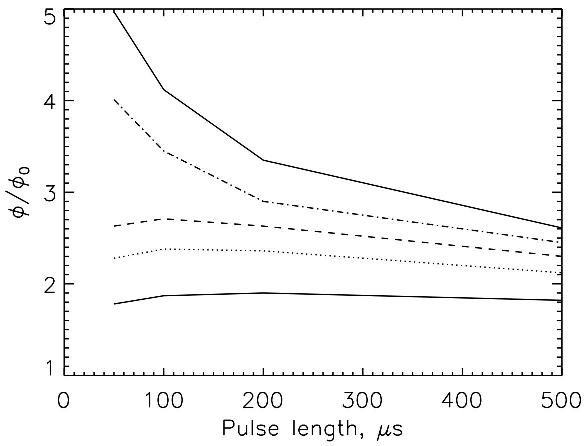

Figure 3. Ratio of the total magnetic flux generated by HF-pulses at 9 MHz and ERP = 95.7 dBW, X-mode for quiet nighttime ionospheric profiles, preheated by a long pulse at f = 4 MHz, and ERP = 88.3 dBW, X-mode to that without preheating (ϕ/ϕ_0) as a function of the short pulse length, for preheating by pulse lengths of 100, 200, 300, 500 s and by a very long pulse (from the bottom to the top respectively).

magnetic field on the ground scales as $B \propto j_0 \propto n_e$ (see equation (1)). Therefore the increased electron density caused by the preheating and shown in Figure 1 leads to the respective increase in the VLF signal.

[13] We conducted a study by varying the heating frequency between the 4–9 MHz using the full HAARP ERP while keeping the preheating pulses same as above. The results indicate that the pre-heating effect optimizes at the highest HF frequency for modulated heating. It is due to the fact that the electron density modification peaks at about 85 km (see Figure 1) favoring heating at high HF frequency due to the reduction of the low altitude self absorption.

[14] A good quantitative measure of the VLF response on the ground is the computed value of the total magnetic field flux defined as $\phi = \int_0^{2t_p} (B_x^2 + B_y^2)dt$ where B_x and B_y correspond to Hall and Pedersen components of the B-field respectively. Figure 3 shows the ratio of the total magnetic flux generated by HF-pulses at 9 MHz, ERP = 95.7 dBW, X-mode, and preheated by a long pulse of 4 MHz, ERP = 88.3 dBW, X-mode, to that of a similar pulse without preheating. The computation was made for a variety of pulse lengths corresponding to VLF frequencies and for three different preheating pulse lengths. The short pulses were generated by HF at 9 MHz frequency, X-mode, and full HAARP ERP. Figure 3 indicates that the strongest increase of the magnetic flux due to preheating can reach 7 dB for an infinite preheating pulse, and reduces with shorter preheating pulses. Furthermore, the effect depends upon the modulation frequency, in a fashion similar to the one discussed by *Papadopoulos et al.* [2005] in the absence of preheating. In fact, short pulses which length matches the electron heating time are more efficient in generating ELF signals than longer pulses.

5. Proof-of-Principle Experiments

[15] Before addressing the practical implementation of the technique and the conduct of proof-of-principle experiments we should examine a role played by the transport processes in the ionosphere with respect to the ionization changes due to electron HF-heating. Taking into account the convection in the horizontal direction equation (3) can be generalized by the following way:

$$\frac{\partial n_e}{\partial t} + \mathrm{v_c}\frac{\partial n_e}{\partial x} = q - \alpha n_e^2 \tag{10}$$

The convection is caused by the $E \times B$ drift and neutral wind resulting in convection velocity given by

$$\mathrm{v_c} = \sqrt{\mathrm{v}_{\mathrm{dr}}^2 + \mathrm{v}_{\mathrm{wind}}^2 + 2\cos\theta\, \mathrm{v_{dr}v_{wind}}} \tag{11}$$

Here $\mathrm{v_{dr}}$ and $\mathrm{v_{wind}}$ are the $E \times B$ drift and wind velocities respectively, while θ is the angle between their directions. Equation (10) can be simplified by taking into account that the spatial scale of the perturbation due to HF-heating is equal to the size of the irradiated spot L, thus we get

$$\frac{\partial n_e}{\partial t} = q - \alpha n_e^2 - \frac{n_e}{L}\mathrm{v_c} \tag{12}$$

[16] Equation (12) shows that the convection reduces changes in n_e due to electron heating, and increases the characteristic timescale required for the electron density to reach its steady state. In fact, the steady state density due to electron heating becomes

$$n_e^{st} = n_o\sqrt{\frac{\alpha_o}{\alpha}}\left\{\sqrt{1 + \frac{1}{4\alpha q \tau_{tr}^2}} - \frac{1}{2\sqrt{\alpha q}\tau_{tr}}\right\} \tag{13}$$

where $n_o\sqrt{\frac{\alpha_o}{\alpha}} = \sqrt{\frac{q}{\alpha}}$ is steady state density reached in the absence of the transport, while the transport timescale $\tau_{tr} = L/\mathrm{v_c}$. Therefore, $n_e^{st} < n_o\sqrt{\alpha_o/\alpha}$. Furthermore, equations (12), (13) show that the transport significantly reduces the increase in the electron density caused by HF-heating, if the transport time is shorter than the timescale required for the density to reach its steady state value τ_{ch} shown.

[17] Assuming that the peak of electron perturbation occurs at about 85 km (see Figure 1 (right)) where $\tau_{\mathrm{ch}} \simeq$ 100 s, and that for the heating frequency of 4 MHz the size of spot L(85 km) $\simeq$ 30 km, we obtain that the transport effect can be neglected if $\tau_{\mathrm{ch}} \ll \tau_{\mathrm{tr}}$, or if $\mathrm{v_c} \ll 300$ m/s. It means that the transport effect is negligible if the E×B drift is caused by a moderate convection field $E_\mathrm{c} \ll 20$ mV/m.

[18] In the opposites case of a strong convection field ($\tau_{\mathrm{ch}} > \tau_{\mathrm{tr}}$) convection limits HF-heating time to τ_{tr} thus reducing the peak changes in the electron density as illustrated by Figure 1. However, the efficiency of ELF generation is proportional to the value of E_c, therefore we expect that the optimal convection field of about 10 mV/m might exist although it has to be confirmed by future experiments.

[19] As a result, in the proposed proof-of-principles experiment the choice of preheating regime is dictated by the ionospheric conditions. At a moderate convection field, which can be detected either by the HAARP ionosonde or by radar, a long pulse of a few hundred seconds, which achieves steady state electron density, can be used for preheating. It will be followed by a modulated heating at

frequencies 1–20 kHz for a few hundred seconds. At a strong convection field a 100–300 s preheating pulse, with length determined by the transport time, is followed by a modulated heating over 100–300 s at modulation frequencies 1–20 kHz. An alternative implementation is to split the HAARP antenna array into two overlapping beams operating at two different frequencies. In this case half of the power of the array is used to maintain the modified density profile while the remaining power is used to modulate the current.

[20] In conclusion, a novel way to increase an efficiency of the ELF/VLF generation by HF-heating of the ionosphere is proposed. As shown by our computer simulations a preheating of the lower ionosphere by a long HF-pulse can increase the peak intensity of the ELF/VLF signal by up to 7 dB. The effect is due to increase of the local electron density caused by a partial suppression of the electron-ion recombination rate by the electron heating. All simulations were made based on the characteristics of the recently updated HAARP facility.

[21] **Acknowledgments.** The work was supported by the ONR Grant NAVY.N0017302C60 and by the ONR MURI Grant 5-28828.

References

Barr, R., and P. Stubbe (1984), ELF and VLF radiation from the "polar electrojet antenna," *Radio Sci.*, *19*, 1111.

Barr, R., and P. Stubbe (1991), ELF radiation from the Tromso "Super Heater" facility, *Geophys. Res. Lett.*, *18*, 1035.

Ferraro, A. J., H. S. Lee, T. W. Collins, M. Baker, D. Werner, F. M. Zain, and P. J. Li (1989), Measurements of extremely low frequency signals from modulation of the polar electrojet above Fairbanks, Alaska, *IEEE Trans. Antennas Propag.*, *37*, 802.

Golyan, S. F., et al. (1982), Ionization change induced in the ionospheric *E* layer by intense radio waves, *Geomagn. Aeron.*, *22*, 553–555.

Gurevich, A. V. (1978), *Nonlinear Phenomena in the Ionosphere*, 370 pp., Springer, New York.

Johnsen, R. (1993), Electron-temperature dependence of the recombination of ions $H_3O^+(H_2O)_n$ with electrons, *J. Chem. Phys.*, *97*, 5390.

McCarrick, M., D. D. Sentman, A. Y. Wong, R. F. Wuerker, and B. Chouinard (1990), Excitation of ELF waves in the Schuman resonance range by modulated HF heating of the polar electrojet, *Radio Sci.*, *25*, 1291.

Milikh, G. M., K. Papadopoulos, M. McCarrick, and J. Preston (1999), ELF emission generated by the HAARP HF-heater using varying frequency and polarization, *Radiophys. Quantum Electr.*, *42*, 728–735.

Mironenko, L. F., V. O. Rapoport, S. N. Mityakov, and D. S. Kotik (1998), Radiation of superluminal irregularities artificially created in the lower ionosphere, *Radiophys. Quantum Electr.*, *41*, 196.

Papadopoulos, K., A. S. Sharma, and C. L. Chang (1989), On the efficient operation of a plasma antenna driven by modulation of ionospheric currents, *Comments Plasma Phys. Control. Fusion*, *13*, 1.

Papadopoulos, K., C. L. Chang, P. Vitello, and A. Drobot (1990), On the efficiency of ionospheric ELF generation, *Radio Sci.*, *25*, 1311.

Papadopoulos, K., T. Wallace, M. McCarrick, G. M. Milikh, and X. Yang (2003), On the efficiency of ELF/VLF generation using HF heating of the auroral electrojet, *Plasma Phys. Rep.*, *29*, 606–611.

Papadopoulos, K., T. Wallace, G. Milikh, W. Peter, and M. McCarrick (2005), The magnetic response of the ionosphere to pulsed HF heating, *Geophys. Res. Lett.*, *32*, L13101, doi:10.1029/2005GL023185.

Rietveld, M. T., and P. Stubbe (2006), Comment on "The magnetic response of the ionosphere to pulsed HF heating" by K. Papadopoulos et al., *Geophys. Res. Lett.*, *33*, L07102, doi:10.1029/2005GL024853.

Rietveld, M. T., H. Kopka, and P. Stubbe (1986), *D*-region characteristics deduced from pulsed ionospheric heating under auroral electrojet conditions, *J. Atmos. Terr. Phys.*, *48*, 311.

Rietveld, M. T., P. Stubbe, and H. Kopka (1987), On the frequency dependence of ELF/VLF waves produced by modulated ionospheric heating, *Radio Sci.*, *24*, 270.

Tripathi, V. K., C. L. Chang, and K. Papadopoulos (1982), Excitation of the Earth-ionosphere waveguide by an ELF source in the ionosphere, *Radio Sci.*, *17*, 1321.

Zhou, H. B., K. Papadopoulos, A. S. Sharma, and C. L. Chang (1996), Electromagneto-hydrodynamic response of a plasma to an external current pulse, *Phys. Plasmas*, *3*, 1484.

G. M. Milikh and K. Papadopoulos, Department of Astronomy, University of Maryland, College Park, MD 20742, USA. (milikh@astro.umd.edu)